Journal of Materials Chemistry C

Strongly luminescent inorganic-organic hybrid semiconductors with tunable white light emissions by doping

Journal:	*Journal of Materials Chemistry C*
Manuscript ID	TC-ART-10-2018-005020.R1
Article Type:	Paper
Date Submitted by the Author:	03-Dec-2018
Complete List of Authors:	Liu, Wei; Shenzhen Polytechnic, Hoffmann Institute of Advanced Materials Banerjee, Debasis; Pacific Northwest National Laboratory, Materials Science Lin, Fang; Shenzhen Polytechnic, Hoffmann Institute of Advanced Materials Li, Jing; Rutgers State Univ

Journal Name

ARTICLE

Strongly luminescent inorganic-organic hybrid semiconductors with tunable white light emissions by doping

Wei Liu[a,b], Debasis Banerjee[b], Fang Lin[a] and Jing Li*[b,a]

A series of copper bromide based inorganic-organic hybrid semiconductors have been synthesized by doping trace amount of a secondary ligand into their parent structures. Upon near-ultraviolet excitation, these structures emit broadband bluish ("cold") to yellowish ("warm") white light. The color temperature can be systematically tuned by controlling the type and amount of the dopant. Our studies show that the observed white emission is emitted directly from the doped sample, not a combined effect from mixed phases. The internal quantum yields (IQYs) of these white-light-emitting hybrids are as high as 68%, which is significantly higher than most of direct white-light-emitting phosphors reported to date. In addition, these copper halide staircase chain based hybrid structures exhibit interesting thermochromic luminescence. The high quantum efficiencies coupled with facile and low-cost synthesis and strong optical tunability of this material group suggests considerable promise for lighting-related applications.

Introduction

The energy-efficient white-light-emitting-diodes (WLEDs) are commonly produced by coating a blue LED chip with blue-excitable phosphors. Such system is regarded as phosphor-converted WLEDs (pc-WLEDs).[1, 2] A simplest pc-WLED makes use of a yellow phosphor, cerium-doped yttrium aluminium garnet (YAG:Ce). However, light emitted from this device typically lacks the lower energy (red) emission, resulting in an elevated correlated color temperature (CCT) that is too "cold" for indoor illumination.[1, 3] An alternative approach is to excite direct white light-emitting phosphor by a near ultraviolet LED chip. Such phosphors are typically a blend of several monochromic emitters. This design has several advantages such as better light quality, facile device fabrication etc.[4-6] However, there are also disadvantages including significant self-absorption and color change due to the decomposition of one component in the blends.[7-10] Beside these issues, nearly all commercial phosphors in today's market contain rare-earth elements (REEs), which bring up potential supply, cost, and environmental issues.[11, 12]

In the recent years, single-phase, non-rare-earth, direct white-light-emitting phosphors have been developed and are attracting increasing attention due to their considerable potential for lighting-related applications.[13-25] For example, II-VI (e.g. Zn, Cd and S, Se) based nano-crystal quantum dots (QDs) of very small size can generate white light.[26-28] However, their internal quantum yields (IQYs) are generally low. Their emissions are highly dependent on the particle sizes which also require complicated synthesis procedures. These drawbacks limit their practical use. Inorganic-organic hybrid semiconductors are a unique family of semiconductor bulk materials that exhibit enhanced properties with respect to their parent structures.[29-36] Unique properties, especially luminescence, have emerged as a result of combining both the inorganic and organic component in a single crystal lattice.[14, 37-40] The structures built on II-VI based semiconductors and alkyl-amines emit white light in their bulk phases. Their IQYs reach 37% upon Mn^{2+} doping.[14, 41, 42] Layered halide perovskites, on the other hand, exhibit intrinsic white light emission with IQY of 9%.[37, 43, 44] However, compared to the IQYs of commercial phosphors that are usually higher than 80 %, the photoluminescence efficiency of these structures needs to be further improved for practical applications.

Our recent studies on I-VII binary metal halide (Cu, Ag and I, Br, Cl) based inorganic-organic hybrid semiconductors demonstrate their strong potential as general lighting phosphors.[38, 45-47] This family of compounds have a number of advantages compared to commercial and other phosphor classes, such as strong luminescence, earth-abundance, REE-free, and facile one-step synthesis. The emission profiles of nearly all of these structures are single-band type, with full width at half maximum (FWHM) of around 100 nm.[48, 49] Broadened emission spectra can be achieved by doping a secondary ligand onto the pristine hybrids.[38] Herein, we report a series of one dimensional (1D) staircase chain-like copper (I) bromide based inorganic-organic hybrid compounds with the general formula 1D-CuBr(pyridine)$_{1-x}$(pyrazine

a. Hoffmann Institute of Advanced Materials, Shenzhen Polytechnic, 7098 Liuxian Blvd, Nanshan District, Shenzhen, 518055, China
b. Department of Chemistry and Chemical Biology, Rutgers University, 610 Taylor Road, Piscataway, NJ, 08854, USA
*Email - jingli@rutgers.edu

derivatives)$_x$ (x<0.01), where pyrazine (*pz*) derivatives are the dopants (Fig. 1). These doped compounds exhibit tunable white light emission as well as significantly enhanced IQYs, a 6-fold improvement compared to previously reported copper iodide based analogues.[38] A comprehensive analysis has been done by varying doping amount and by modifying dopants with different functional groups. The results demonstrate that the light temperature of doped compounds is adjustable. Bluish ("cold") to yellowish ("warm") white light from single crystals of these structures have been achieved, indicating the white light is emitted directly from the doped bulk materials (Fig. 2). Moreover, we have observed reversible thermochromic behavior on all white-light-emitting compounds. This behavior has never been reported previously for copper halide staircase chain based structures. The advantages of high IQYs, facile synthesis and optical tunability make this type of phosphors promising candidates as lighting phosphors, and their thermochromic behavior may leads to new applications.

emit strongly in the visible light region and their emission colors range from blue to green. Their emission spectra are all single-band type, with an average of full width at half maximum (FWHM) of around 100 nm. Their emission energies are in trend with their band gap values and the LUMO energies of the incorporated ligands. The internal quantum yields (IQYs) of **1**-**4** have been determined at room temperature, and the values obtained with 360 nm as the excitation wavelength are 56%, 48%, 27% and 21% for **1**, **2**, **3** and **4**, respectively. These results demonstrate that the varying functional groups on the *py* ligands significantly influence the quantum yield of the hybrid structures. Electron donating groups, such as methyl groups, enhance the emission, while electron-withdrawing groups, such as chlorine or bromine, lower the emission efficiency. The structures' band gaps, emission energies, IQY and ligand LUMO energies are highly related to each other and are in agreement with our previous studies on 1D-CuI(*L*). The optical properties of these structures can be tuned by ligand design and selection.
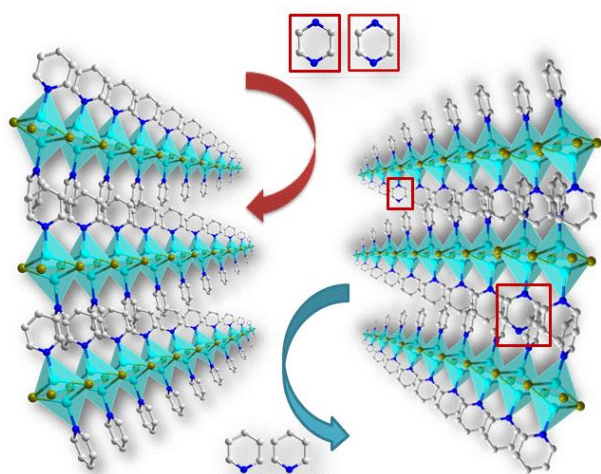

Figure 1. Schematic Illustrating the ligand doping approach in designing white emitting 1D-CuBr(*py*)$_{1-x}$(*pz*)$_x$ compounds.

Results and discussion

Attempts to synthesize copper bromide based hybrid semiconductors lead to the formation of compounds **1**-**4**. They are all copper bromide staircase chain based structures (Figs. S4-S9). Important crystallographic data of these compounds are listed in Table 1. Their phase purities have been evaluated and confirmed by elemental analysis (Table S1). The optical absorption spectra for compounds **1**-**4** were recorded at room temperature and converted to the Kubelka-Munk function (Fig. S12). Their band gaps were estimated by their absorption edges, and are 3.1, 2.8, 2.7 and 2.5 eV, respectively. This trend corresponds with the decreasing LUMO energies of the organic ligands in the structures, which are -1.039, -1.120, -1.473 and -1.492 eV for *3,5-dm-py*, *py*, *3-Cl-py* and *3-Br-py*, respectively (Table S2). As shown in Fig S15 and Table S3, these structures
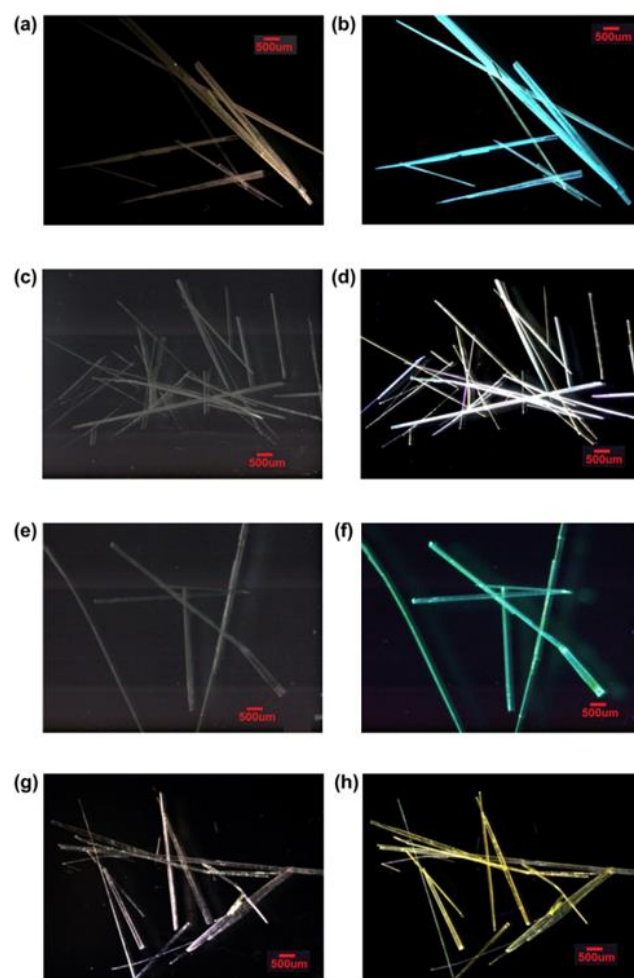

Figure 2. Single crystals of **2** (a), **2c** (c), **2f** (e), **2g** (g) under natural light and **2** (b), **2c** (d), **2f** (f), **2g** (h) under UV light (365nm).

Compound **2** or 1D-CuBr(*py*) (space group P2$_1$) was chosen as the parent structure for doping study.[50] It exhibits intense blue-green emission (λ$_{em}$ = 495 nm) under near-UV excitation (λ$_{ex}$ = 360 nm) with an IQY of 48%. In the case of parent structure, adding trace amount of *pz* afforded doped products 1D-CuBr(*py*)$_{1-x}$(*pz*)$_x$ (x < 0.01) (compounds **2a**-**2d**). The PXRD analysis confirmed that the crystal structure of these doped samples remain to be the same (Fig. 3a). Photoluminescence measurements of the doped samples show that their emissions change significantly compared to that of the parent structure (Fig. 3c). The blue-green emission band from their parent structure remains in the higher energy (HE) region, while a second band emerges in the spectra located at lower energy (LE) region resulted from doping. The HE and LE bands combine to give a broad emission spanning over the entire visible light region (400-700 nm). Centimeter-long single crystals of doped samples were obtained by layering approach and all optical measurements of the doped samples were from single-phased samples. It was observed that the white light is emitted directly from the single crystals, suggesting it is a bulk property of the material. We also grinded the single crystals of 1D-CuBr(*py*)$_{1-x}$(*pz*)$_x$ (x = 0.0012) into fine powders. No changes in emission were observed before and after grinding, confirming that the luminescence is not a surface property.

The absorption spectra for doped structures **2a**-**2h** were collected and all exhibit a single, sharp absorption edge, indicating they are single-phase compounds (Fig. S13). All of the doped compounds have nearly the same band gap values as that of their parent structure 1D-CuBr(*py*). The possible impurities from dopant under this condition are 2D-CuBr(*L*)$_{0.5}$ (Fig. S5b), which have band gaps around 2.0 eV—significantly lower than that of 1D-CuBr(*py*). [51] However, no absorption at the lower energy part was observed in any of the spectra of doped structures. This confirms that the second bidentate ligands have been doped into the parent structure, and are not forming a second impurity phase. Further increasing the doping level to x = 0.01 leads to the formation of a second phase, identified by the UV-vis absorption spectra as a new absorption band appeared in addition to that of 2D-CuBr(*pz*)$_{0.5}$ (Fig. S14). Therefore, we keep the doping amount significantly lower than 1 % to ensure their single phase purity.

By varying the doping level of *pz*, from 0.05 % to 0.32 % molar ratio to that of *py*, the peak positions of the HE and LE bands remain unchanged while their intensities vary based on the doping level. With increasing doping amount, we observe a gradual intensity decrease of the HE band along with an intensity increase of the LE band. When the doping level is reaches 0.32%, the HE is almost totally quenched, resulting in an intense "yellowish" white light.

The intense blue-green emission of the parent structure 1D-CuBr(*py*) is primarily attributed to a combination of metal-to-ligand charge-transfer (MLCT) and halide-to-ligand charge transfer (XLCT) luminescence mechanism, as confirmed by Density Functional Theory (DFT) calculations (Fig. 3b and S11). The band gap and emission energy of this type of structures are correlated to the LUMO energy of the ligand. Further calculation of LUMO energies shows that *pz* has distinctly lower energy (-1.857 eV) compared to that of *py* (-1.120eV), indicating the parent ligand and the dopant might be responsible to the dual emissions (Table S2). To understand this, we kept the parent ligand *py*, and changed the *pz* to *pz* derivatives (*2-et-pz*, *2-me-pz*, *2-Cl-pz*, *2-Br-pz*) with different LUMO energies. Single crystals of 2a-2h were obtained with these dopants, and PXRD analysis along with UV-vis absorption experiment was conducted to confirm their phase correctness and purity. Based on their photoluminescence measurements, all compounds exhibit a two-band type spectrum (Fig. S16). The emission energies of HE band remain constant for all of them, proving that the HE band is from the parent ligand *py*. The energies of LE band however, changes accordingly based on the LUMO energies of the dopants, providing strong evidence that the LE band is originated from the dopants.

Table 1. Summary of crystal data of new 1D-CuBr(*L*) structures (*L* = py functionalized ligand).

Compound	1D-CuBr(*3,5-dm-py*) (**1**)	1D-CuBr(*3-Cl-py*) (**3**)	1D-CuBr(*3-Br-py*) (**4**)
Empirical Formula	C$_7$H$_9$BrCuN	C$_5$H$_4$BrClCuN	C$_5$H$_4$Br$_2$CuN
FW	250.60	256.99	301.44
Space Group	C2/c	P2$_1$/n	P2$_1$/n
a (Å)	13.910(17)	8.7438(19)	8.720(9)
b (Å)	15.111(18)	3.9296(9)	3.933(4)
c (Å)	8.107(10)	21.002(5)	21.11(2)
A(°)	90.00	90.00	90.00
B(°)	99.455(17)	100.837(3)	100.603(13)
γ(°)	90.00	90.00	90.00
V (Å^3)	1681(4)	708.7(3)	711.6(12)
Z	8	4	4
T (K)	298(2)	298(2)	298(2)
λ(Å)	0.71073	0.71073	0.71073
R$_1$	0.0396	0.0306	0.0479
wR$_2$	0.0973	0.0817	0.1207
CCDC #	1506745	1506742	1506741

Furthermore, the relative intensities of the HE and LE band under various excitation wavelength have been studies (Fig. 3d). The observation of their excitation-wavelength dependent emissions suggests that the HE band and the LE band are from isolated luminous centers. The time-resolved PL measurements were conducted on the doped sample with the excitation wavelength of 360 nm at the emission maximum of the two bands. The lifetime values for 495 nm and 550 nm emissions are 17.5 µs and 26.3 µs, respectively (Fig. 3e). The difference of the lifetime values reflect their different excited states.

Table 2. Summary of the composition and optical properties of white-light-emitting structures.

| #	Dopant	Doping amount	Band gap (eV)	λ_{em} (nm) (298K)	λ_{em} (nm) (77K)	IQYs (%) 360nm	CIE	CRI	CCT (K)
2a	*pz*	0.05	3.0	494 (HE) 545 (LE)	494	60	0.34, 0.41	68.4	5792
2b	*pz*	0.07	3.0	494 (HE) 545 (LE)	494	64	0.35, 0.42	67.0	5024
2c	*pz*	0.12	3.0	484 (HE) 545 (LE)	494	61	0.39, 0.43	67.2	3888
2d	*pz*	0.32	3.0	494 (HE) 545 (LE)	494	54	0.42, 0.46	58.0	3658
2e	*2-et-pz*	0.12	3.0	494 (HE) 520 (LE)	494	68	0.26, 0.36	65.4	4259
2f	*2-me-pz*	0.12	3.0	494 (HE) 525 (LE)	494	66	0.28, 0.37	65.5	3940
2g	*2-Cl-pz*	0.12	3.0	494 (HE) 556 (LE)	494	35	0.43, 0.42	77.2	3697
2h	*2-Br-pz*	0.12	3.0	494 (HE) 575 (LE)	494	24	0.44, 0.40	75.6	3360
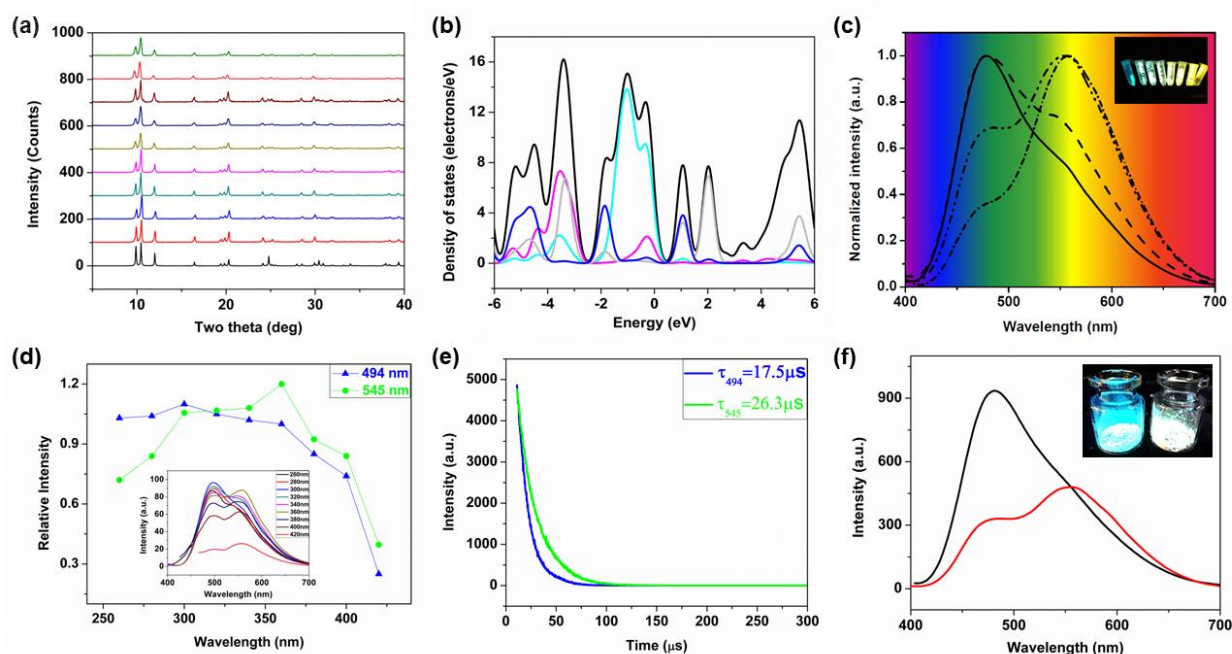
Figure 3. (a) PXRD patterns of parent and doped structures of 1D-CuBr(py) compared with simulated pattern. From bottom to top: simulated **2**, as made **2**, as made **2a**-**2h**. The dopant concentrations are listed in Table 2. (b) Calculated density of states (DOS) of 1D-CuBr(*py*) (**2**) by DFT method: total DOS (black); Cu 3d orbitals (light blue); Br 4p orbitals (pink); C 2p orbitals (grey); N 2p orbitals (blue). (c) Photoluminescence spectra of **2a** (solid), **2b** (dash), **2c** (dash dot dot) and **2d** (short dash dot). Inset: Photo images of the doped samples under UV light. Samples from left to right: parent 1D-CuBr(*py*), 0.004%, 0.008%, 0.02%, 0.05%, 0.07%, 0.12%, 0.32% *pz* doped 1D-CuBr(*py*). λ_{ex} = 365 nm. (d) Relative intensities of the HE band at 494 nm (blue) and LE band at 545 nm (green) respectively for **2c**, as a function of excitation wavelengths. The intensity of the HE band at 360 nm is set to 1. Inset: PL spectra of **2c** with various excitation wavelengths. (e) Luminescence decay spectra of **2c** at 494 nm (blue) and 545 nm (green). λ_{ex} = 360 nm. (f) PL spectra of **2c** at room temperature (red) and at 77K (black). Inset: Images of **2c** taken immediately after removing sample from liquid nitrogen (left) and at room temperature (right).

The temperature-dependent emission spectra of doped samples show that they all display thermochromic behavior (Fig. 3f). The intensity of LE band was completely quenched when the sample was dipped in liquid nitrogen (77 K), while the intensity of HE band becomes much stronger. After removing the crystals from liquid nitrogen, the initial emission intensities of the two bands are regained as the sample temperature returns to RT, indicating that the thermochromic luminescence is fully reversible. Though thermochromic behavior for copper halide cubane cluster-based hybrid materials has been well studied and is attributed to short Cu-Cu bond distances (smaller than 2.8 Å),[48, 52-54] as far as we are aware, such behavior has not been reported for staircase chain based structures. For example, a typical cubane cluster, 0D-$Cu_4I_4(py)_4$, emits LE (yellow) emission at room temperature originated from "cluster centered" (CC) luminescence, and at low temperature (77 K), the LE emission is quenched and the HE (blue) emission emerges as a combination of metal-to-ligand and halide-to-ligand charge transfer (MLCT and XLCT).[48] The LE band emission in doped 1D-CuBr(py) samples is similar to that of cubane based structures, indicating they might also be attributed to CC luminescence mechanism. Single crystal X-ray diffraction is not capable to provide an answer as the doping level is too low to form an ordered structure. We also noted that the dopants must be multidentate ligands in order to achieve the broadening effect of the spectra. Other multidentate ligands, including pyrimidine (*pm*) and 1,3,5-triazine (*tz*), exhibit a similar behavior as *pz* derivatives (Fig. S17). However, when replacing these dopants with monodentate ligands having lower LUMO energies, such as *3-cyano-py* and *4-cyano-py* (Table S2), no broadening effect was observed. The full understanding of the broaden effect through doping is still limited, and further in-depth investigation of the luminescence mechanism is now underway.

The direct application of these white-lighting-emitting materials is their use as lighting phosphors. The quality of the white light from these phosphors is readily tunable by selecting suitable dopants and doping amount. The performance of doped compounds as lighting phosphors were evaluated by IQY measurements, CIE (International Commission on Illumination) color coordinates, Color Rendering Index (CRI) and Correlated Color Temperature (CCT) under the excitation of near-ultraviolet light (365 nm) and the results are summarized in Table 2. It is interesting to observe that the IQYs of most doped structures are higher than that of their parent structure, with the highest IQY value of 68% for compound **2e**. Compared to other reported direct white light emitting phosphors which generally suffer from low IQYs, most of these compounds have IQYs higher than 60%. More interestingly, their color temperature can also be tuned, from bluish (cold) to yellowish (warm) white light, as evident from their CCT values (Fig. 4). The current commercial white light LEDs made from YAG:Ce produce "cold" white light with CCT values higher than 5000 K which may not be suitable for indoor illumination.[1] The color temperatures of the doped 1D-

CuBr(py), on the other hand, range from 3360 K to 5792 K, making these materials usable under various environment.
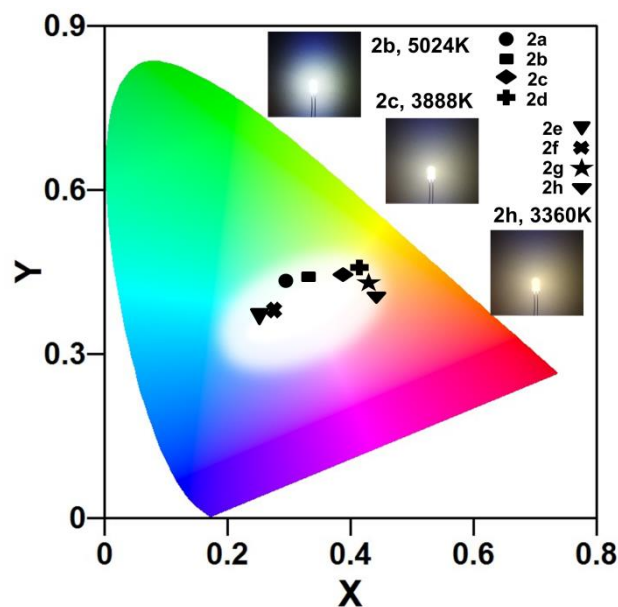

Figure 4. CIE coordinates of all white-light-emitting structures. Inset: photos of the LED bulbs under working condition.

Moreover, the water stability of these materials ensures their solution processability. Using commercial binder they can be easily coated onto different substrates. Prototype WLED bulbs were fabricated by coating 5 mm 365 nm LED chips with doped samples having various CCT values. These bulbs display white light from "cold" to "warm" as their CCT values decrease from 5024 K to 3360 K (Fig. 4).

Experimental

Materials. CuBr (98%, Alfa Aesar), KBr (>99%, Alfa Aesar), acetonitrile (>99%, Alfa Aesar), pyridine (*py*, >99%, Alfa Aesar), 3,5-dimethylpyridine (*3,5-dm-py*, >98%, Alfa Aesar), 3-chloropyridine (*3-Cl-py*, 99%, Alfa Aesar), 3-bromopyridine (*3-Br-py*, >98%, Alfa Aesar), pyrazine (*pz*, 98%, Alfa Aesar), 2-ethyl-pyrazine (*2-et-pz*, 98%, Alfa Aesar), 2-methyl-pyrazine (*2-me-pz*, 98%, TCI), 2-chloro-pyrazine (*2-Cl-pz*, 98%, Alfa Aesar), 2-bromo-pyrazine (*2-Br-pz*, 98%, TCI), sodium salicylate (SS, 99%, Merck).

General procedures for the synthesis of undoped structures (1) to (4). Single crystals of 1D-CuBr(*3,5-dm-py*) (**1**), 1D-CuBr(*py*) (**2**), 1D-CuBr(*3-Cl-py*) (**3**) and 1D-CuBr(*3-Br-py*) (**4**) were acquired by a layered method. The reactions were conducted in glass vials or tubes (Fig. S1-S3). The bottom, middle and top layers were CuBr/KBr saturated aqueous solution, acetonitrile, and ligand in ethanol, respectively. The crystals formed in the middle layer over 3-5 days at room temperature. Pure phase powder samples were obtained by direct mixing of CuBr (0.1mmol) in saturated KI solution (2.0 ml) with ligand (0.1mmol) in ethanol (2.0 ml). The pure phase powder generally formed immediately after stirring.

General procedures for the synthesis of doped structures. The syntheses of doped compounds 1D-CuBr(*py*)$_{1-x}$(*pz derivatives*)$_x$ (x<0.01) are similar as that of their parent structures. A stock solution of 10^{-4} M *pz* derivatives in ethanol was pre-prepared. Single crystals of doped structures were obtained by layered method. The ligand in ethanol solution was made by mixing the *pz* derivatives stock solution with *py* in various molar ratios, from 0% to 1.0% of *py*. Pure phase powder samples were made by directly mixing the ligand solution with the CuBr in KI saturated solution while stirring at room temperature. The doped structures obtained are 1D-CuBr(*py*)$_{1-x}$(*pz*)$_x$ (x = 0.0005, **2a**; x = 0.0007, **2b**; x = 0.0012, **2c**; x = 0.0032, **2d**) and 1D-CuBr(*py*)$_{0.9988}$(*pz derivatives*)$_{0.0012}$, (*pz derivatives = 2-et-pz* (**2e**); *2-me-pz* (**2f**); *2-Cl-pz* (**2g**), *2-Br-pz* (**2h**). All products were collected by filtration and dried in vacuum oven for further characterization.

Single crystal X-ray diffraction (SXRD) and powder X-ray diffraction (PXRD) analysis. Single crystal X-ray diffraction data of **1**, **3**, **4** were collected at low temperature (100 K) on a Bruker-AXS smart APEX I CCD diffractometer with graphite-monochromated MoKα radiation (λ = 0.71073 Å) at room temperature. The structures were solved by direct methods and refined by full-matrix least-squares on F2 using the Bruker SHELXTL package. The structures were deposited in the Cambridge Structural Database (CSD), and the file numbers are 1506741, 1506742, 1506745. A summary of the crystal data of all five compounds are given in Table 1. PXRD patterns of these structures were obtained from a Rigaku Ultima-IV automated diffraction system with Cu Kα radiation. Measurements were made in a 2θ range of 3-50°. The data were collected at room temperature with a step of 0.02° (2θ) and a counting time of 0.2 s/step. The operating power was 40 kV/44 mA.

Characterizations and DFT calculations. Optical diffuse reflectance spectra were measured at room temperature on a Shimadzu UV-3600 spectrophotometer. Data were collected in the wavelength range of 300-1000 nm and % reflectance was converted to the Kubelka-Munk function. Photoluminescence (PL) measurements were carried out on a Varian Cary Eclipse spectrophotometer at room temperature. Thermogravimetric (TG) analyses were performed on a computer-controlled TG Q5000 analyzer (TA Instrument) with a ramp rate of 10 °C/min from room temperature to 400 °C. The internal quantum yield (IQY) was measured on samples in powder form using a C9920-03 absolute quantum yield measurement system (Hamamatsu Photonics) with a 150 W xenon monochromatic light source and 3.3 inch integrating sphere. Sodium salicylate (99%, Merck) was used as the standard with an IQY value of 60% when excited at 360 nm. The standard was measured to be 65%, indicating experimental error of less than 10%. Luminescence lifetime was measured by the FLS920 Edinburgh fluorimeter (Edinburgh Instruments, Livingston, United Kingdom) with a microsecond μF900 xenon flash lamp as the excitation resource and by time-correlated single photon counting. Instrumental response function (IRF) was applied if the instrumental response could not be neglected for shorter lifetimes.

Conclusions

In summary, a series of copper bromide inorganic-organic hybrid semiconductors have been synthesized and structurally characterized. Upon doping by trace amount of a second, multidentate ligand, they exhibit bright and tunable white light emissions. The color quality of their white emission can be precisely controlled and tuned by varying the dopant and doping amount, generating a range of "cold" to "warm". All doped compounds also exhibit thermochromic behavior as a function of temperature. This work provides the first example of a systematic study that demonstrates dopant effect on the photoluminescence of copper bromide based hybrid structures.

Conflicts of interest

There are no conflicts to declare.

Acknowledgements

Notes and references

1.   X. Huang, *Nat Photon*, 2014, 8, 748-749.
2.   Y. H. Kim, P. Arunkumar, S. H. Park, H. S. Yoon and W. B. Im, *Materials Science and Engineering: B*, 2015, 193, 4-12.
3.   H. Zhu, C. C. Lin, W. Luo, S. Shu, Z. Liu, Y. Liu, J. Kong, E. Ma, Y. Cao, R.-S. Liu and X. Chen, *Nat Commun*, 2014, 5.
4.   B. Song, Y. Zhong, S. Wu, B. Chu, Y. Su and Y. He, *Journal of the American Chemical Society*, 2016, 138, 4824-4831.
5.   N. Horiuchi, *Nat Photon*, 2010, 4, 738-738.
6.   M. Yoshihiko, K. Masahiro and N. Suguru, *Semiconductor Science and Technology*, 2014, 29, 084004.
7.   N. C. George, K. A. Denault and R. Seshadri, *Annual Review of Materials Research*, 2013, 43, 481-501.
8.   A. Moazzam, C. Soma, N. Angshuman, K. Akshay, S. Sameer, S. Chakraborty and D. D. Sarma, *Nanotechnology*, 2007, 18, 075401.
9.   P. Thiyagarajan, M. Kottaisamy and M. S. R. Rao, *Journal of Physics D: Applied Physics*, 2006, 39, 2701.
10.   H. J. Yu, K. Park, W. Chung, J. Kim, B.-h. Chun and S. H. Kim, *Polym. J*, 2009, 41, 1076-1079.
11.   B. Sprecher, I. Daigo, S. Murakami, R. Kleijn, M. Vos and G. J. Kramer, *Environmental Science & Technology*, 2015, 49, 6740-6750.
12.   A. Tukker, *Environmental Science & Technology*, 2014, 48, 9973-9974.
13.   Y.-C. Liao, C.-H. Lin and S.-L. Wang, *Journal of the American Chemical Society*, 2005, 127, 9986-9987.
14.   W. Ki and J. Li, *Journal of the American Chemical Society*, 2008, 130, 8114-8115.
15.   T. Ogi, H. Iwasaki, A. B. D. Nandiyanto, F. Iskandar, W. N. Wang and K. Okuyama, *Journal of Materials Chemistry C*, 2014, 2, 4297-4303.
16.   T. Nakajima, M. Isobe, Y. Uzawa and T. Tsuchiya, *Journal of Materials Chemistry C*, 2015, 3, 10748-10754.

17. Z.-Y. Mao, F. Wang, J.-J. Chen and D.-J. Wang, *Journal of the American Ceramic Society*, 2015, 98, 3856-3862.
18. W. Liu, K. Zhu, S. J. Teat, G. Dey, Z. Shen, L. Wang, D. M. O'Carroll and J. Li, *Journal of the American Chemical Society*, 2017, 139, 9281-9290.
19. W. Liu, Y. Fang and J. Li, *Advanced Functional Materials*, 2018, 28, 1705593.
20. M.-S. Wang, S.-P. Guo, Y. Li, L.-Z. Cai, J.-P. Zou, G. Xu, W.-W. Zhou, F.-K. Zheng and G.-C. Guo, *Journal of the American Chemical Society*, 2009, 131, 13572-13573.
21. Z.-F. Liu, M.-F. Wu, S.-H. Wang, F.-K. Zheng, G.-E. Wang, J. Chen, Y. Xiao, A. Q. Wu, G.-C. Guo and J.-S. Huang, *Journal of Materials Chemistry C*, 2013, 1, 4634-4639.
22. G.-E. Wang, G. Xu, M.-S. Wang, L.-Z. Cai, W.-H. Li and G.-C. Guo, *Chemical Science*, 2015, 6, 7222-7226.
23. M.-S. Wang and G.-C. Guo, *Chemical Communications*, 2016, 52, 13194-13204.
24. N.-N. Zhang, C. Sun, X.-M. Jiang, X.-S. Xing, Y. Yan, L.-Z. Cai, M.-S. Wang and G.-C. Guo, *Chemical Communications*, 2017, 53, 9269-9272.
25. M.-S. Wang, G.-C. Guo, W.-T. Chen, G. Xu, W.-W. Zhou, K.-J. Wu and J.-S. Huang, *Angewandte Chemie International Edition*, 2007, 46, 3909-3911.
26. T. E. Rosson, S. M. Claiborne, J. R. McBride, B. S. Stratton and S. J. Rosenthal, *Journal of the American Chemical Society*, 2012, 134, 8006-8009.
27. M. J. Bowers Ii, J. R. McBride, M. D. Garrett, J. A. Sammons, A. D. Dukes Iii, M. A. Schreuder, T. L. Watt, A. R. Lupini, S. J. Pennycook and S. J. Rosenthal, *Journal of the American Chemical Society*, 2009, 131, 5730-5731.
28. A. D. Dukes, P. C. Samson, J. D. Keene, L. M. Davis, J. P. Wikswo and S. J. Rosenthal, *The Journal of Physical Chemistry A*, 2011, 115, 4076-4081.
29. X. Huang, J. Li and H. Fu, *Journal of the American Chemical Society*, 2000, 122, 8789-8790.
30. X. Huang and J. Li, *Journal of the American Chemical Society*, 2007, 129, 3157-3162.
31. C. R. Kagan, D. B. Mitzi and C. D. Dimitrakopoulos, *Science*, 1999, 286, 945-947.
32. D. B. Mitzi, S. Wang, C. A. Feild, C. A. Chess and A. M. Guloy, *Science*, 1995, 267, 1473-1476.
33. X. Zhang, M. Hejazi, S. J. Thiagarajan, W. R. Woerner, D. Banerjee, T. J. Emge, W. Xu, S. J. Teat, Q. Gong, A. Safari, R. Yang, J. B. Parise and J. Li, *Journal of the American Chemical Society*, 2013, 135, 17401-17407.
34. X. Huang, M. Roushan, T. J. Emge, W. Bi, S. Thiagarajan, J.-H. Cheng, R. Yang and J. Li, *Angewandte Chemie International Edition*, 2009, 48, 7871-7874.
35. Z.-J. Zhang, G.-C. Guo, G. Xu, M.-L. Fu, J.-P. Zou and J.-S. Huang, *Inorganic Chemistry*, 2006, 45, 10028-10030.
36. G.-E. Wang, G. Xu, B.-W. Liu, M.-S. Wang, M.-S. Yao and G.-C. Guo, *Angewandte Chemie International Edition*, 2016, 55.
37. E. R. Dohner, E. T. Hoke and H. I. Karunadasa, *Journal of the American Chemical Society*, 2014, 136, 1718-1721.
38. X. Zhang, W. Liu, G. Z. Wei, D. Banerjee, Z. Hu and J. Li, *Journal of the American Chemical Society*, 2014, 136, 14230-14236.
39. C. Sun, G. Xu, X.-M. Jiang, G.-E. Wang, P.-Y. Guo, M.-S. Wang and G.-C. Guo, *Journal of the American Chemical Society*, 2018, 140, 2805-2811.
40. C. Sun, M.-S. Wang, P.-X. Li and G.-C. Guo, *Angewandte Chemie International Edition*, 2017, 56, 554-558.
41. X. Fang, M. Roushan, R. Zhang, J. Peng, H. Zeng and J. Li, *Chemistry of Materials*, 2012, 24, 1710-1717.
42. M. Roushan, X. Zhang and J. Li, *Angewandte Chemie International Edition*, 2012, 51, 436-439.
43. E. R. Dohner, A. Jaffe, L. R. Bradshaw and H. I. Karunadasa, *Journal of the American Chemical Society*, 2014, 136, 13154-13157.
44. M. D. Smith and H. I. Karunadasa, *Accounts of Chemical Research*, 2018, 51, 619-627.
45. W. Liu, Y. Fang, G. Z. Wei, S. J. Teat, K. Xiong, Z. Hu, W. P. Lustig and J. Li, *Journal of the American Chemical Society*, 2015, 137, 9400-9408.
46. Z. Liu, M. F. Qayyum, C. Wu, M. T. Whited, P. I. Djurovich, K. O. Hodgson, B. Hedman, E. I. Solomon and M. E. Thompson, *Journal of the American Chemical Society*, 2011, 133, 3700-3703.
47. Z. Liu, J. Qiu, F. Wei, J. Wang, X. Liu, M. G. Helander, S. Rodney, Z. Wang, Z. Bian, Z. Lu, M. E. Thompson and C. Huang, *Chemistry of Materials*, 2014, 26, 2368-2373.
48. P. C. Ford, E. Cariati and J. Bourassa, *Chemical Reviews*, 1999, 99, 3625-3648.
49. K. Tsuge, Y. Chishina, H. Hashiguchi, Y. Sasaki, M. Kato, S. Ishizaka and N. Kitamura, *Coordination Chemistry Reviews*, 2016, 306, Part 2, 636-651.
50. P. Healy, J. Kildea, B. Skelton and A. White, *Australian Journal of Chemistry*, 1989, 42, 93-105.
51. J. Pospisil, I. Jess, C. Nather, M. Necas and P. Taborsky, *New J. Chem.*, 2011, 35, 861-864.
52. S. Perruchas, C. Tard, X. F. Le Goff, A. Fargues, A. Garcia, S. Kahlal, J.-Y. Saillard, T. Gacoin and J.-P. Boilot, *Inorganic Chemistry*, 2011, 50, 10682-10692.
53. S. Perruchas, X. F. Le Goff, S. Maron, I. Maurin, F. Guillen, A. Garcia, T. Gacoin and J.-P. Boilot, *Journal of the American Chemical Society*, 2010, 132, 10967-10969.
54. Q. Benito, X. F. Le Goff, S. Maron, A. Fargues, A. Garcia, C. Martineau, F. Taulelle, S. Kahlal, T. Gacoin, J.-P. Boilot and S. Perruchas, *Journal of the American Chemical Society*, 2014, 136, 11311-11320.
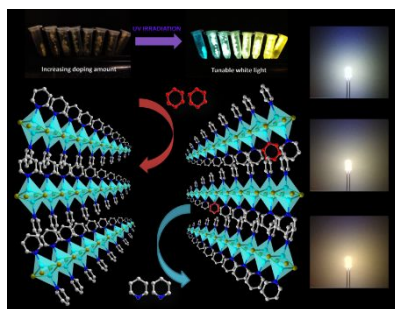
Tunable white light emissions from copper bromide based inorganic-organic hybrid semiconductors have been achieved by doping.